Specific heat and magnetic interactions in $NdCrO_3$

Fernando Bartolomé and Juan Bartolomé
ICMA, CSIC–Universidad de Zaragoza, 50009 Zaragoza, Spain

Miguel Castro
ICMA, CSIC–Universidad de Zaragoza, 50009 Zaragoza, Spain
and Departamento de Ciencia de Materiales y Fluídos, CPS, Universidad de Zaragoza, 50017 Zaragoza, Spain

Julio J. Melero
ICMA, CSIC–Universidad de Zaragoza, 50009 Zaragoza, Spain
and Departamento de Ingeniería Eléctrica, CPS, Universidad de Zaragoza, 50017 Zaragoza, Spain
(Received 3 February 2000)

The specific heat of $NdCrO_3$ in the thermal range from 0.3 to 300 K is presented. The magnetic ordering of Cr ions at $T_N = 219 \pm 1$ K is observed, as well as the spin reorientation transition (SRT) at $T_{SRT} = 34.2 \pm 0.5$ K. The specific heat of the isostructural nonmagnetic compound $LaGaO_3$ has been subtracted, allowing us to separate and quantify the different magnetic contributions to the specific heat in $NdCrO_3$. The exchange coupling constant for the Cr-Cr interaction is found to be $|J_{Cr}|/k_B = 21.7(7)$ K. The fitting of the Schottky contribution from the thermal depopulation of the Nd^{3+} $^4I_{9/2}$ ground multiplet allows us to propose a crystal-field energy-level scheme which is in agreement with the available neutron-scattering spectral lines. The intensity of the Nd-Cr magnetic interaction is obtained. Finally, we show that the strength of the Nd-Cr interaction in this compound is of the same order of magnitude as that found in other Nd orthoperovskites, namely, in $NdFeO_3$, despite the different Zeeman splitting of the Nd ground doublet in both compounds.

I. INTRODUCTION

Rare-earth oxide compounds with perovskite structure are receiving renewed attention in connection with the discovery of high-T_c superconductivity and, more recently, colossal magnetoresistance. It is quite remarkable that these compounds, which almost all have a rather simple structure (usually orthorhombic), provide a rich variety of electronic and magnetic phenomena depending on the atoms involved, the interatomic distances and the bonding strength. In particular, RMO_3 are model systems to investigate the interactions between the two types of magnetic atoms (R is a rare earth, and M a $3d$ or $4d$ metal). Those interactions follow the hierarchy of M-M, M-R, and R-R in descending order according to their strength. The $NdMO_3$ family attracted our attention because it has a wide range of M magnetic and nonmagnetic substitution with the same structure (space group D_{16}^{2h}). Nd^{3+} ions occupy a low-symmetry position, and its $^4I_{9/2}$ ground multiplet is fully split into five Kramers doublets by the C_s-m low-symmetry crystal field. Moreover, each doublet is split by the Zeeman effect due to the internal field H_{Nd-M}.

In some previous studies, Nd-Nd interaction was assumed to be so weak that the collective magnetic ordering of the Nd sublattice was regarded as impossible.[1] It was a surprise to find that $NdGaO_3$, where the Nd-Nd interaction is in isolation, indeed orders magnetically at $T_N = 1.05$ K, as evidenced by a sharp lambda anomaly in its specific heat.[2] Later we observed similar ordering temperatures in $NdCoO_3$ (where Co ions are in low-spin non-magnetic state),[3] $NdScO_3$,[4,5] and $NdInO_3$.[4,6] We found that while $NdCoO_3$ presents the same c_z magnetic structure as $NdGaO_3$, $NdScO_3$ and $NdInO_3$ order in a different magnetic mode $g_y a_x$ (magnetic modes are given in Bertaut's notation[7]). The substitution of M by a magnetic $3d$ transition metal, such as Fe, Ni, or, Cr leads to magnetic ordering of the M sublattice at high temperature, namely, $T_{N1} = 690$, 200, and 220 K, respectively. Below T_{N1} the M sublattice magnetization induces an effective magnetic field on the Nd sublattice due to the Nd-M interaction, $H_{\text{Nd-}M}$, which tends to polarize it in a definite magnetic mode, compatible with the M order,[7] as clearly observed by neutron diffraction in $NdFeO_3$,[8] $NdNiO_3$,[9] and $NdCrO_3$.[10] This effect is observable in heat-capacity measurements since it splits the ground doublet of the Nd^{3+} ion, giving rise to a Schottky anomaly.[3,11] The Nd moments thus behave as a paramagnetic system in an (staggered) internal field. However, at a sufficiently low temperature, the weak Nd-Nd interaction may show that the Nd sublattice actually undergoes a long-range cooperative ordering transition, as evidenced by a small λ peak at $T_{N2} \sim 1$ K superimposed on the Schottky anomaly in $NdFeO_3$ and $NdNiO_3$.[3] Finding a T_{N2} similar in value to that found in the M nonmagnetic substitutions allows us to conclude that the Nd-Nd interaction is of similar intensity throughout the whole series of $NdMO_3$ compounds.

In contrast to Fe and Ni compounds, no λ peak is observed in the specific heat of $NdCrO_3$, and the Schottky maximum appears at a higher temperature (~ 11 K in the chromite[11] instead of ~ 2.2 K in the ferrite and niquelate[3]). We could rationalize these differences by means of a mean-field model which predicts that when the ratio of intensities of Nd-M and Nd-Nd interactions is larger than a certain

critical value the cooperative order of the Nd system is inhibited.[3] One concludes that a relatively strong effective M-R interaction is present in the $NdCrO_3$ compound. This is unexpected, since the rather low M sublattice ordering temperature implies that M-M interaction is lower than that in $NdFeO_3$. Such a intriguing behavior turns $NdCrO_3$ into an interesting system.

The Cr spins order in $NdCrO_3$ at $T_{N1}=220$ K (Ref. 12) in an antiferromagnetic G_zF_x (Γ_2) mode. The Cr magnetic moments undergo a spin reorientation transition (SRT) to the G_y (Γ_1 mode) at $T_{SRT}=35.1$ K. Neutron-diffraction measurements[10] allowed us to conclude that Nd-Cr interaction was able to polarize the Nd sublattice at temperatures below T_{SRT}, giving rise to the above-mentioned Schottky anomaly. In spite of an improper correction for the lattice contribution to the specific heat, the splitting of the Nd^{3+} ground doublet was found to be $\Delta_g/k_B=27$ K.[11] A more quantitative approach was attempted by Hornreich and co-workers,[13,14] who performed, among other experiments, optical spectroscopy measurements on $NdCrO_3$ as a function of temperature. Their results show a Zeeman splitting of the Nd^{3+} ground doublet of $\Delta_g/k_B=25.9$ K at 34 K, undergoing a discontinuous drop to $\Delta_g/k_B=23.6$ K when heating just above T_{SRT}. With these values, the magnetic specific heat due to the ground doublet alone was predicted below $T<50$ K. The unavailability of experimental data above 20 K, on the one hand, and the lack of a proper determination of other contributions to the specific heat, on the other hand (lattice, excited Nd doublets, and spin waves of the Cr system), avoided a comparison with experiment. Such a comparison is one of the objectives of the present work.

The energy of the first excited doublet was also optically measured as $E_e/k_B=114\pm7$ K.[13,14] Later, Shamir *et al.* determined $\Delta_g/k_B=28$ K and $E_e/k_B=127$ K by inelastic neutron scattering at 4.2 K.[15] The line centered at E_e was too wide to observe the splitting Δ_e of the excited doublet.

Hornreich *et al.* proposed[13] that Δ_g is mainly due to Nd-Cr interaction above T_{SRT}, while below that temperature Nd-Nd interaction becomes significant, originating the aforementioned discontinuous behavior of Δ_g. However, our systematic study of $NdMO_3$ oxides has shown that Nd-Nd interaction is very weak, $|J_{Nd}|/k_B\approx0.8$ K, inducing appreciable changes in Δ_g only below ~5 K. Moreover, it has been stated that Nd-Cr interaction is extremely strong in $NdCrO_3$[13,16] compared to other rare-earth–transition-metal couplings in orthoperovskites.

Our goal with this work is to perform a complete calorimetric investigation of $NdCrO_3$, studying the different contributions to the specific heat. This will allow us to test the cited prediction as well as to study the strength of the Nd-Cr interaction. To separate the several contributions to the specific heat of $NdCrO_3$ (magnetic contributions due to the Cr^{3+} system, thermal depopulation of the split levels of Nd, etc.) we have measured the specific heat of the isostructural, nonmagnetic $LaGaO_3$ compound in a wide range of temperatures.

II. EXPERIMENTAL DETAILS

The specific-heat measurements in the range 0.3 K $<T<$ 6 K were performed in a fully automated quasiadiabatic calorimeter[17] refrigerated by adiabatic demagnetization of a paramagnetic salt,[18,19] using the heat-pulse technique and germanium thermometry in the whole temperature range. The absolute accuracy of the instrument has been estimated to be about 1%. The calorimetric data between 4 and 275 K were obtained in a commercial Sinku-Riko ac calorimeter. The relative values obtained by this technique have a precision of 0.1%. They were scaled to the absolute values measured with a DSC7 Perkin Elmer calorimeter from 100 K up to room temperature.

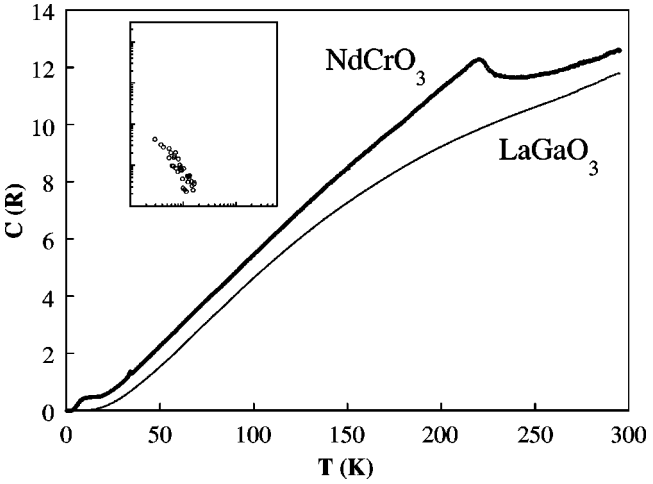

FIG. 1. Specific-heat curves of $NdCrO_3$ (symbols) and $LaGaO_3$ (line). The upper inset shows $NdCrO_3$ specific heat on a double-log scale. The hyperfine contribution becomes evident in $NdCrO_3$ below $T=1$ K. The lower inset show the same data on a linear scale, evidencing the spin reorientation transition peak and the low-temperature Schottky hump.

$NdCrO_3$ and $LaGaO_3$ powder samples were obtained by sintering a mixture of the binary oxides. For the low-temperature experiment about 0.5 g of $NdCrO_3$ were mixed with Apiezon N grease to achieve a good thermal contact even at the lowest temperatures between the sample and the calorimetric set (heater and thermometer). To perform the ac calorimetric measurements, we profited of a single crystal of $NdCrO_3$, kindly provided by A. M. Kadomtseva, to measure in the range of temperatures 4 K $<T<$ 300 K. For the $LaGaO_3$ measurements, a thin pellet of ≈10 mg of powdered sample was prepared.

III. EXPERIMENTAL RESULTS

The experimental specific heat curves of $NdCrO_3$ and $LaGaO_3$ are presented in Fig. 1. $NdCrO_3$ data range between 0.25 and 300 K, while $LaGaO_3$ data are shown only above 4.2 K for clarity. The upper inset of Fig. 1 shows the lowest-temperature region in a double-log plot. The increase of C for decreasing temperature below 1 K reveals the high-temperature tail of the hyperfine contribution from Nd, already observed in $NdGaO_3$.[2,3,20] The data below $T=40$ K are shown in the lower inset of Fig. 1 on a linear scale. In this plot, the small peak due to the spin reorientation transition taking place at $T=34$ K is clearly visible.

In order to evaluate the magnetic contributions to the $NdCrO_3$ specific heat, we have calculated the difference specific heat curves by subtraction of the nonmagnetic $LaGaO_3$,

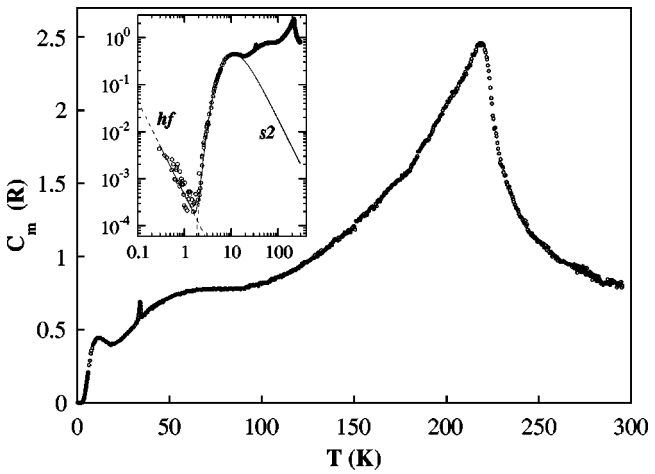

FIG. 2. Magnetic specific heat of $NdCrO_3$, C_m. The inset shows the same data on a double-log scale. The fitted hyperfine (hf) and two-level Schottky ($s2$) contributions are also shown.

after scaling by a Lindemann factor[21] of 1.036 the temperature of the experimental curves of $LaGaO_3$. This correction to the lattice contribution takes account of the difference in mass of the Nd and Cr atoms respect to the La and Ga atoms. The resulting curve, shown in Fig. 2, is the magnetic specific heat, which will be referred as C_m ($NdCrO_3$ is an insulator in the whole temperature range, thus no electronic contribution to the specific heat needs to be considered). As previously, the inset shows the same data in a double-log scale, allowing one to appreciate the details of the curve in the low-temperature region. A direct inspection of the curve evidences the presence of four main contributions or features: the hyperfine contribution below 1 K, the electronic Schottky contribution from thermal depopulation of the ground $^4I_{9/2}$ multiplet of Nd between 2 K up to the higher temperatures, the spin reorientation peak at $T=34.2\pm0.5$ K, and the λ peak due to antiferromagnetic ordering of the Cr magnetic moments ($S=3/2$) centered at $T=219\pm1$ K.

A. Hyperfine contribution

At very low temperatures, C_m can be well described by the addition of two contributions, $C_m=C_{hf}+C_{Sch}$: the high-temperature tail of the theoretical hyperfine contribution, C_{hf}, originated by the nonzero magnetic moments of ^{143}Nd, ^{145}Nd, and ^{53}Cr nuclei, summed to the low-temperature part of the electronic Schottky contribution, C_{Sch}. The nuclear spin of ^{143}Nd and ^{145}Nd is $I=7/2$ in both cases, with 12.2% and 8.3% natural abundance respectively, while $I=3/2$ for ^{53}Cr with 9.5% natural abundance. One can calculate the mean square of the effective nuclear moment for the natural abundance of the active isotopes of Cr and Nd, $\overline{\mu_{eff}^2}$, yielding $0.229\mu_N^2$ for Nd and $0.035\mu_N^2$ for Cr. With these effective nuclear moments one can conclude that the Cr hyperfine contribution is about one order of magnitude smaller than the Nd one, and comparable to the dispersion in the data below 1 K. Thus only the Nd contribution is taken into account in the calculation of C_{hf}. Within this approximation, the hyperfine field on Nd, H_{hf}, can be calculated. The estimated error in H_{hf} due to neglecting the Cr contribution is smaller than the uncertainty from systematic and statistical errors. The subsystem of Nd nuclear spins contributes to the specific heat in the form of a weighted Schottky curve due to the thermal depopulation of the eight equally spaced levels (with splitting Δ_{hf}). The electronic contribution can be described below ~12 K by a two-level Schottky curve, because $\Delta_g \gg E_e$, so it allows one to treat the ground doublet as isolated. The fitting of the available data to the sum of those two contributions yields $\Delta_{hf}/k_B=0.022(5)$ K and $\Delta_g/k_B=27.1$ K. The same high-temperature approximation used for the magnetization Brillouin function may be applied to the hyperfine high-temperature specific heat,

$$C_{hf}/R=\frac{\overline{\mu_{eff}^2}\cdot H_{hf}^2}{3k_B^2T^2}, \tag{1}$$

and the best fit of the data to this power law yields $C_{hf}/R=4.6(5)\times10^{-4}T^{-2}$. The fitted curves are shown in the inset of Fig. 2 as dashed lines, labeled hf and *s2* for the hyperfine and electronic contributions, respectively, and their sum is shown as a full line. The fit of the hyperfine contribution allows one, through Eq. (1) to determine the Nd hyperfine field in $NdCrO_3$, $H_{hf}=2.1(2)$ MOe.

B. Contributions below T_{N1}

To separate the Nd and Cr contributions to C_m is a complicated task. However, a separation of the different contributions is possible following a step-by-step process. At the end, the total entropy content provides a method to ensure the soundness of the procedure.

As already stated, the rounded maximum at $T_{max}=11.5(5)$ K is predominantly due to the two-level Schottky curve caused by the split Nd ground doublet. Its fit is the first step of the procedure, which immediately gives the energy splitting $\Delta_g/k_B=27.15(8)$ K, in excellent agreement with neutron inelastic experiments (28 K).[15] Once Δ_g is fixed, our second step only involves C_m below $T=30$ K, which can be well described by a Schottky curve considering just two Nd doublets, split by Δ_g and Δ_e, with their centers separated by the energy E_e.

The results of this analysis are depicted in Fig. 3, where C_m below 30 K is compared with the calculated two-doublet Schottky contribution obtained with different values of E_e and Δ_e. In each case, Δ_g/k_B has been fixed to 27.15 K, as determined above. Three values reported in the literature for E_e/k_B (see Sec. I) have been used in the three panels: 97 K (top), 114 K (medium), and 127 K (low). Within each panel, curves *a*, *b*, and *c* are calculated with $\Delta_e/k_B=0$, 27, and 50 K, respectively. $\Delta_e=0$ corresponds to an unsplit first excited doublet, $\Delta_e/k_B=27$ K was the result obtained from the analysis of Ref. 13, and $\Delta_e/k_B=50$ K has been included to evidence the change induced by a large Δ_e in C_{Sch}. Two conclusions can be derived from the analysis of Fig. 3: (a) the only curves compatible with C_m are *a* and *b* with $E_e/k_B=127$ K, in very good agreement with neutron scattering experiments by Shamir *et al.*[15]; and (b) the curves with $\Delta_e/k_B=0$ and 27 K are very similar, especially for larger values of E_e. This reflects the rather poor sensibility of the specific heat to Δ_e, as far as it remains small with respect to E_e. In fact, curves *a* and *b*, with $E_e/k_B=127$ satisfactorily reproduce C_m below 20 K, where higher-

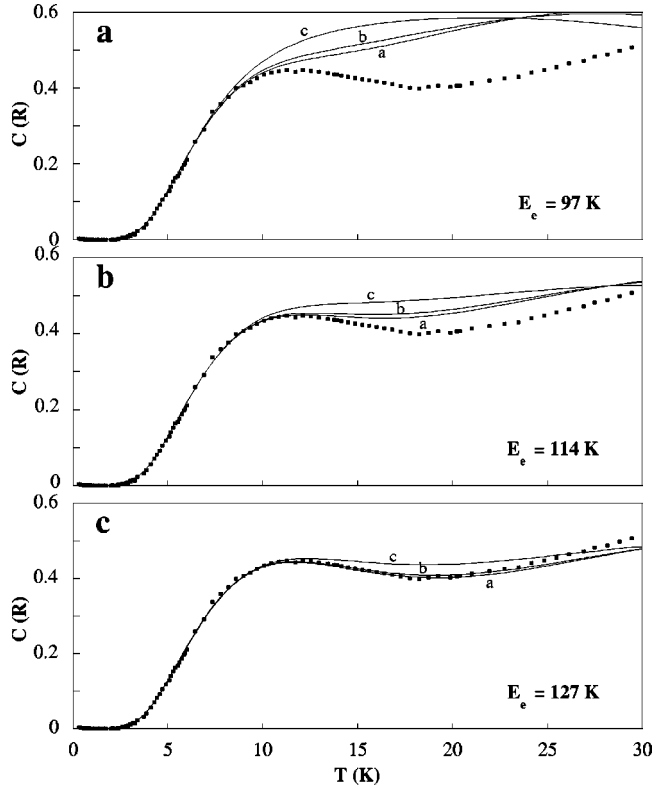

FIG. 3. Results of the analysis of C_m below 30 K, where the experimental data are compared with the calculated two-doublet Schottky contribution obtained with different values of E_e and Δ_e (a, b, and c curves of each panel). See the text for details.

energy levels do not appreciably contribute to the specific heat. As $\Delta_e/k_B = 27 \pm 3$ K is an experimental result[13] and its influence in the analysis of C_m is almost negligible, we decided to keep it as a constant in our subsequent fitting procedure.

The third step takes into account the contributions from the three higher Nd doublets, as well as the magnetic contribution from the Cr subsystem. In order to reduce the number of free parameters, we have kept fixed the energy of the fifth doublet, E_5, which should be similar to that of the Nd^{3+} ion in $NdGaO_3$, $E_5/k_B = 784$ K.[4,22] This value is also very similar to that found in a wide group of Nd oxides.[23] Moreover, in the temperature range of interest, $T < 300$ K, C_m is not sensitive to changes of E_5.

Next we have considered the contribution of the Cr-ordered sublattice up to ~ 150 K. This is due to antiferromagnetic spin-wave excitations in a three-dimensional magnetic lattice, which is known to follow a T^3 law.[24] We have then fitted C_m up to 150 K, considering two additive contributions: a Schottky curve C_{Sch} due to the five Nd Kramers doublets, with only E_3 and E_4 as free parameters, plus the $C_{sw}/R = a_{sw}T^3$ term. Therefore, the excited doublets are treated as being unsplit by $H_{Nd\text{-}Cr}$. However, the analysis of Fig. 3 suggests that from the fitting of the specific heat only, we can expect, at most, to obtain the energy of the center of gravity of each doublet. The fit is excellent in the temperature range $2K < T < 150$ K, as shown in Fig. 4. The parameter values obtained are $E_3/k_B = 233(5)$ K, $E_4/k_B = 504(5)$ K, and $a_{sw} = 2.05(5) \times 10^{-7}$ K^{-3}. The crystal-field level scheme is coherent with those found experimentally in other Nd oxides, such as $NdFeO_3$[25] [$E_3/k_B = 255(20)$ K and $E_4/k_B = 520(20)$ K], $NdGaO_3$ (Refs. 4 and 20) ($E_3/k_B = 260$ K and $E_4/k_B = 615$ K), and $NdNiO_3$ (Ref. 26) ($E_3/k_B = 220$ K and $E_4/k_B = 650$ K). Figure 4 also shows separately C_{Sch} (dotted line) and C_{sw} (dashed line). A scheme in Fig. 4 summarizes the Nd energy levels originating the calculated C_{Sch}.

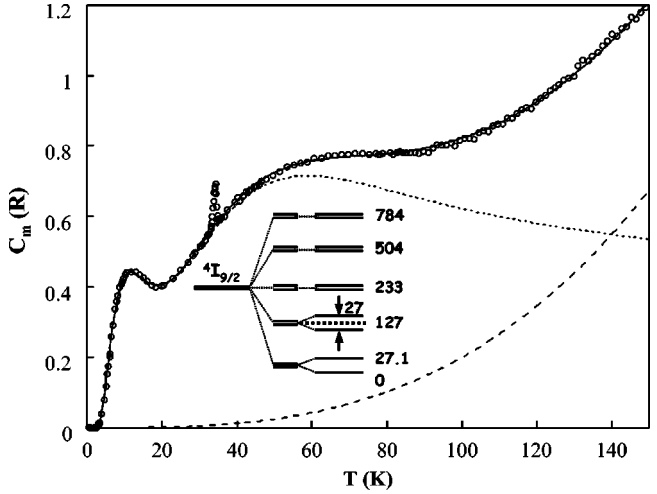

FIG. 4. Magnetic specific heat of $NdCrO_3$ below 150 K (open symbols). The fitted curve (solid line) is the sum of the Schottky curve from Nd $^4I_{9/2}$ (dotted line) and the magnonic specific heat of the Cr subsystem (dashed line). The crystal-field energies derived from the fit is shown in the scheme. For the sake of clarity, only one half of the data is shown.

C. Specific heat of the Cr subsystem

Since the Cr^{3+} ions form a slightly distorted simple cubic magnetic lattice of $S = 3/2$ spins, a simplified model could be used to calculate the Cr-Cr interaction exchange constant from the magnonic specific heat, C_{sw}. To do so we have used the expression for C_{sw} at moderately low temperatures for antiferromagnetic magnons in a s.c. lattice with Heisenberg-like interactions.[24] This approach only takes into account the isotropic interaction, neglecting the antisymmetric and anisotropic terms, but, on one hand, it should give a reasonable value for the order of magnitude of the Cr-Cr exchange and, on the other, the expression for C_{sw} in a more detailed model is not available, to our knowledge. The numerical expression[27,28] for the specific heat within this degree of approximation is

$$C_{sw}/R = 13.7\left(\frac{k_B T}{12JS}\right)^3, \qquad (2)$$

which allows us to extract the value $|J_{Cr}^{sw}|/k_B = 22.4(5)$ K from the best fit given above for C_{sw}.

The Néel temperature and the high-temperature tail of the magnetic ordering λ peak allow us to use two other methods to evaluate $|J_{Cr}|/k_B$, by means of the preditions obtained from the series expansion for the isotropic Heisenberg model with arbitrary spin and crystal lattice by Rushbrooke and Wood.[29] The assumption of the isotropic Hamiltonian is justified by the magnetic susceptibility measurements along the three axes of a single crystal of $NdCrO_3$[13] which show no

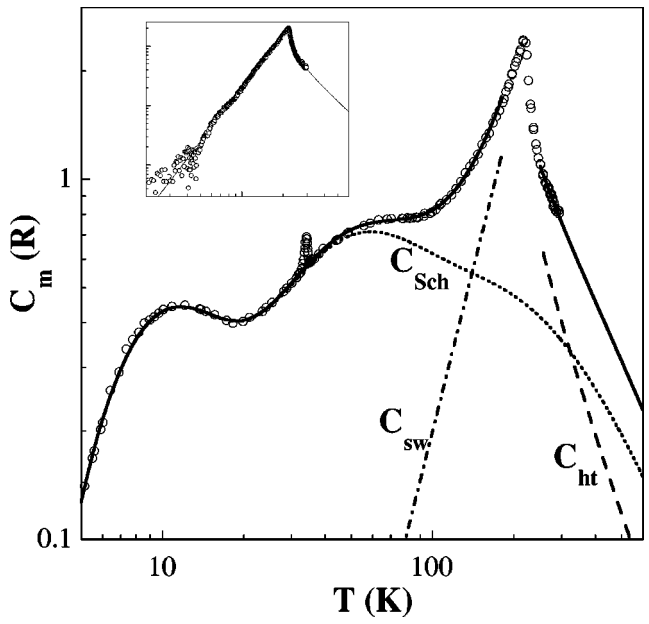

FIG. 5. Magnetic specific heat of $NdCrO_3$ (open symbols) on a double-log scale. For the sake of clarity, only a part of the data is shown. The three separate contributions to the calculated C_m (solid line) are shown; Nd $^4I_{9/2}$ Schottky, C_{Sch} (dotted line), magnonic contribution of the Cr subsystem, C_{sw} (dash-dotted line), and s.c. $S=3/2$, isotropic Heisenberg high-temperature specific heat, C_{ht} (dashed line). The inset show the data on a double-log scale, once C_{Sch} has been subtracted, isolating the Cr magnetic contributions (except for the spin reorientation transition peak at $T=34$ K).

appreciable anisotropy above 150 K. The studies of the magnon-assisted Cr emission spectra on $YCrO_3$, $LuCrO_3$, and $GdCrO_3$ (Ref. 30) also corroborate this approximation, as the experimental results do not evidence any magnetic anisotropy at high temperatures. Therefore, in the paramagnetic region, at temperatures high enough to avoid the critical regime, C_m can be well described by the sum of two contributions $C_m=C_{Sch}+C_{ht}$: the high temperature part of the electronic Schottky contribution, C_{Sch}, already determined by the low-temperature analysis and kept fixed now, plus the high-temperature expansion for the specific heat of a simple cubic, $S=3/2$, isotropic Heisenberg Hamiltonian,

$$C_{ht}/R=\frac{2z(S(S+1))^2}{3\theta^2}\left(1+\sum_{n=1}^{5}\frac{c_n}{\theta^n}\right) \tag{3}$$

where z is the number of nearest neighbors (6 for the s.c. lattice), $\theta=k_BT/J$ and c_n are the expansion coefficients, given in Ref. 29 up to $n=5$. The best fit of C_m above 250 K is shown in Fig. 5, yielding the result $|J_{Cr}^{ht}|/k_B=21.6(5)$ K. Figure 5, one double-log scale, shows the three separate contributions to the calculated C_m (solid): C_{Sch} (dotted line), C_{sw} (dash-dotted line), and C_{ht} (dashed line). Only one-tenth of the data is shown in Fig. 5 for the sake of clarity. The inset of Fig. 5 shows the result of subtracting C_{Sch} from the experimental C_m, isolating the contributions due to Cr ions. C_{sw} and C_{ht} are also shown.

Rushbrook and Wood[29] give a third, semiempirical way to evaluate the isotropic exchange constant of the Heisenberg Hamiltonian for cubic lattices from the transition temperature. After their results, the relation

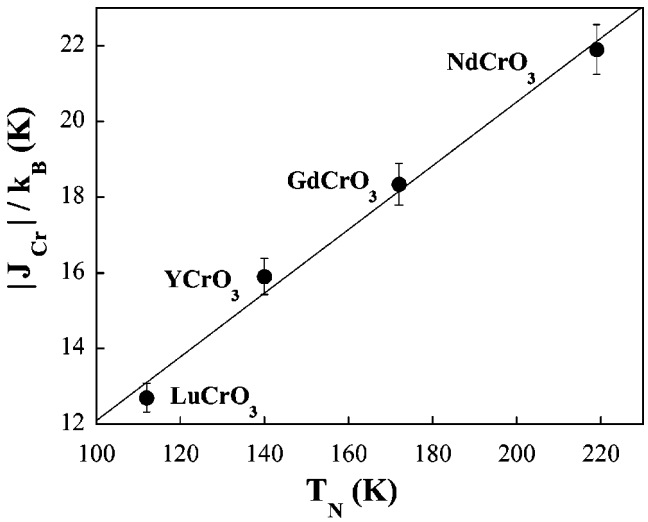

FIG. 6. $|J_{Cr}|/k_B$ as a function of T_N for $LuCrO_3$, $YCrO_3$, $GdCrO_3$ (from Ref. 30), and $NdCrO_3$ (this work).

$$\frac{k_BT_c}{J}=(z-1)(0.579S(S+1)-0.072) \tag{4}$$

holds, which, together with the shift of the magnetic singularity in antiferromagnetic systems,[29]

$$\frac{T_N-T_c}{T_c}\simeq\frac{0.65}{zS(S+1)}, \tag{5}$$

allows one to obtain the value $|J_{Cr}^{T_{N1}}|/k_B=21.0(1)$ K, consistent with the value obtained from the high-T series. T_{N1} is completely independent of our analysis of the specific heat (namely the lattice contribution subtraction); hence its consistency with $|J_{Cr}^{ht}|/k_B$ and $|J_{Cr}^{sw}|/k_B$ (which are strongly dependent on the separation of contributions) is a guarantee of the correctness of our treatment. The dispersion on the $|J_{Cr}|/k_B$ values ($\pm5\%$) gives a rough estimate of the confidence level of the obtained crystal field energies.

We may compare the $|J_{Cr}|/k_B$ values with the values obtained for other rare-earth orthochromites. Van der Ziel and Van Uitert[30] reached $|J_{Cr}|/k_B=12.7$, 15.9, and 18.3 K for $LuCrO_3$, $YCrO_3$, and $GdCrO_3$, with $T_{N1}=112$, 140, and 170 K, respectively. In Fig. 6 we plot $|J_{Cr}|/k_B$ as a function of T_N for different compounds. A linear relation between them is shown notwithstanding the different methods used to determine the exchange constants. The differences have been directly related to different Cr-Cr distances, Cr-O-Cr angles, and the cell volume in the studied compounds.[31] The verification of the linear relation between the Néel temperature and the exchange constant for the Cr systems is another test of the consistency of our calorimetric analysis of $NdCrO_3$.

D. Entropy

The expected total magnetic entropy from the electronic contributions in the whole temperature range is given by the Cr ($S=3/2$) plus the Nd ground-state multiplet ($J=9/2$), i.e., $S/R=(\ln(10)+\ln(4))\approx3.69$. The experimental value,

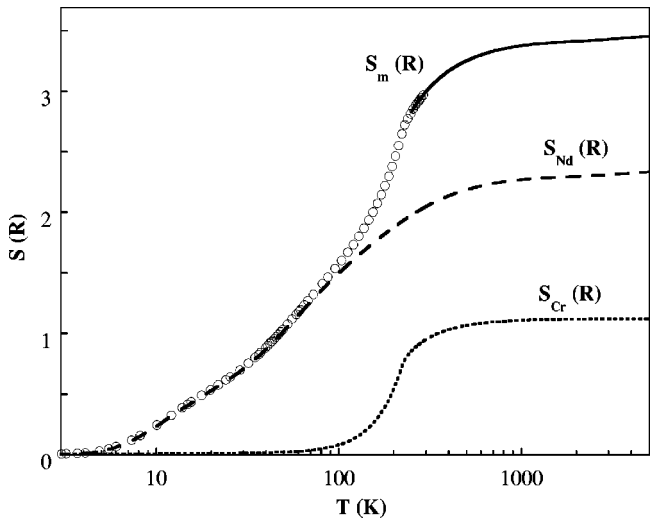

FIG. 7. Magnetic entropy (shown in a semilogarithmic scale) obtained from numerical integration of the experimental C_m/T data below 300 K (○, only 20% of the points are shown for clarity) and from extrapolation of the calculated contributions till $T=5000$ K (solid line). The entropy curves for the Cr (dotted line) and Nd (dashed line) subsystems are also plotted. The top y axis has been plotted at the theoretical expected $S/R=3.69$ value.

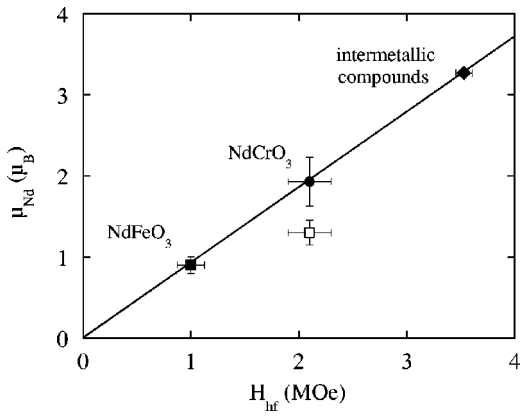

FIG. 8. Magnitude of the Nd effective magnetic moment, $|\mu_{Nd}|$, plotted against the hyperfine field H_{hf} for several Nd systems. The data for $NdFeO_3$ (■) are from Ref. 8. The intermetallic systems (♦) include Nd_2Fe_{17}, $NdFe_{11}Ti$ (Ref. 42), $Nd_2Fe_{14}B$ (Ref. 43), and $Nd_{0.1}Gd_{0.9}$ (Ref. 44). For $NdCrO_3$ we have plotted the H_{hf} obtained in this work together with the two published values for $|\mu_{Nd}|$, $1.3\mu_B$ from Ref. 10 (□), and $1.93\mu_B$ from Ref. 32 (●), which obviously fits within the empirical linear relation between H_{hf} and $|\mu_{Nd}|$.

obtained by numerical integration between 2 and 295 K of the C_m/T data points, is $S_e/R=3.0(1)$. The study of the magnetic contributions presented above allows one to extrapolate C_m to higher temperatures. Beyond the self-consistency of the $|J_{Cr}|/k_B$ values discussed above, the separation of C_m into several contributions should render a proper value for the magnetic entropy extrapolated to $T\rightarrow\infty$.

Figure 7 shows, on a semilogarithmic scale, the magnetic entropy obtained from numerical integration of the experimental C_m/T data (thick line). At higher temperatures, integration of the calculated specific heat yields a value of $S_m(\infty)/R=3.47$, which is only 6% lower than the expected value 3.69. To give a graphic idea of the amount of the entropy defect, the top y axis has been plotted at $S/R=3.69$. The entropy curves for the Cr and Nd subsystems are also plotted. The 6% difference between the expected entropy and the obtained entropy indicates a slight overestimation of the lattice contribution which, due to the structure of our analysis, is fully addressed to the Cr subsystem [S_{Nd} was obtained from the calculated Schottky contribution and, consequently, $S_{Nd}(\infty)/R=\ln(10)$ exactly]. In fact, the entropic defect is of the same order of magnitude as the dispersion on $|J_{Cr}|/k_B$. By inspection of Eqs. (2) and (3) one can see that slightly increasing the global value of the Cr specific heat should decrease $|J_{Cr}^{sw}|/k_B$ while increasing $|J_{Cr}^{ht}|/k_B$; i.e., it should further reduce the already small dispersion in the Cr exchange constant, reinforcing the self-consistency of the obtained results.

IV. DISCUSSION

A. Hyperfine field and Nd magnetic moment

The fit of the Nd hyperfine contribution described in Sec. III A yields a hyperfine field $H_{hf}=2.1(2)$ M Oe. Recently, low-temperature neutron-diffraction experiments on $NdFeO_3$ allowed us to obtain separately Nd H_{hf} and its electronic magnetic moment μ_{Nd}.[8] The ratio H_{hf} to μ_{Nd} in $NdFeO_3$ ($H_{hf}/\mu_{Nd}=1.1\pm0.2$ M Oe/μ_B) was found to be coincident with that of a wide series of intermetallic compounds[8] ($H_{hf}/\mu_{Nd}=1.08\pm0.02$ M Oe/μ_B). Two different values are available in literature for μ_{Nd} in $NdCrO_3$ at 4.2 K: $1.3\mu_B$,[10] giving $H_{hf}/\mu_{Nd}=1.6\pm0.2$ M Oe/μ_B; and the more recent and accurate $1.9\pm0.3\mu_B$,[32] which results in $H_{hf}/\mu_{Nd}=1.15\pm0.25$ M Oe/μ_B. This later value is in excellent agreement with the given ratio for other Nd compounds, as shown by the linear relation shown in Fig. 8, where μ_{Nd} is plotted against H_{hf} for the cited systems. We want to stress the result $\mu_{Nd}^{NdCrO_3}>2\mu_{Nd}^{NdFeO_3}$. This is very important when considering the intensity of Nd-M interactions in those compounds, as Δ_g, which gives a measure of the interaction intensity over the Nd ion, is directly proportional to μ_{Nd}.

B. Spin reorientation transition

In $NdCrO_3$, the high-temperature $\Gamma_2(F_x,C_y,G_z)$ configuration of the Cr spin system discontinuously changes into the low-temperature $\Gamma_1(A_x,G_y,C_z)$ configuration[16,13,33] at T_{SRT}. Our experiment provides a calorimetric detection of this transition in $NdCrO_3$, with $T_{SRT}=34\pm0.3$ K. From the discontinuity of Δ_g/k_B in this spectroscopic data (from 23.6 K above T_{SRT} to 25.9 K below the transition), Hornreich and Yaeger predicted that the specific heat due to the ground Nd doublet should present a discontinuity of 0.02 R at T_{SRT}, with the sharp anomaly characteristic of a first-order transition superimposed onto the step.

To compare this prediction (full line in Fig. 9) with our experimental results, we had to extract the contribution of the ground doublet to C_m. To do this, we subtracted, from the Nd contribution shown in Fig. 4 ($C_{Sch}=C_m-C_{sw}$), the part which is due to depopulation from the excited levels to

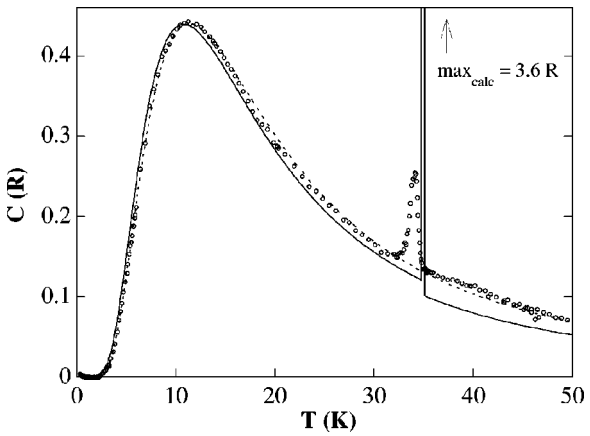

FIG. 9. Specific-heat Schottky contribution of the Nd ground doublet, compared to the Hornreich's prediction (solid line) presenting a discontinuity of $0.02R$ at T_{SRT} and a sharp anomaly characteristic of a first-order transition. The theoretical curve obtained from our fit, with $\Delta_g/k_B=27.15$ K (dotted line), is also shown.

the ground doublet. This contribution from ''higher levels'' (C_{hl}) can simply be obtained as the specific heat caused by the level scheme depicted in Fig. 4 if the ground doublet were degenerated and placed at the energy of the center of gravity of the split (actual) doublet.[34] The result of this final subtraction, $C_{Sch}-C_{hl}$, is the data shown in Fig. 9 (open symbols). The peak corresponding to the first-order SRT becomes evident in this figure. Measurements upon heating or cooling reveal a rather small thermal hysteresis of ~ 0.2 K. The entropy change related to this transition is very small, as it occurs in an almost fully ordered Cr sublattice. Its first-order character is rather evident in magnetization measurements, due to the disappearance of the weak ferromagnetic moment of Γ_2 when cooling below T_{SRT}.[16,13] The small effect on the specific heat contrasts with the abrupt change observed in the magnetization.

Figure 9 shows that the data are very well described by a temperature-independent two-level Schottky curve with $\Delta_g/k_B=27.15$ K (dotted line), which below T_{SRT} is essentially the curve predicted by Hornreich and Yaeger, shifted to lower T (in Ref. 13, $\Delta_g/k_B=25.9$ K is used). The discontinuity on Δ_g is not visible in our data, as no step is observed at T_{SRT}. The discontinuity on the spectroscopic data was interpreted as the appearance in the low-temperature configuration (Γ_1) of a contribution of about 2 K to Δ_g originated by the Nd-Nd interaction. As we have stated above, our systematic low-temperature study of the NdMO_3 series shows that Nd-Nd interaction is by far too weak to induce a splitting of 2 K at temperatures as high as T_{SRT}. This effect can be estimated qualitatively in a similar way to that used for $NdFeO_3$ in Ref. 8 [see Eq. (6) in Sec. IV C] by using diffraction intensities due to Nd polarization. At T_{SRT}, the splitting induced by Nd-Nd interaction is no larger than 0.2 K.[35]

The values of Δ_g above and below T_{SRT} used by Hornreich and Yaeger to calculate the step in the specific heat were also used to calculate the energy change of the spin reorientation transition: $\Delta U/R=0.37(2)$ K. The value obtained from direct integration of our data, once the two-level Schottky curve has been subtracted, is $\Delta U/R=0.15(2)$ K, a very similar value to that found experimentally in $ErCrO_3$ (Ref. 36) (0.12 K), though quite a bit smaller than the predicted value. The difference between the calculated and experimental ΔU also indicates that the effect of Nd-Nd interaction was overestimated at T_{SRT} in Ref. 13.

C. Nd-Cr interaction

To rationalize the effect of Nd-Nd and Nd-Cr interactions, we have used a simple model developed for $NdFeO_3$.[8] The model properly describes both regimes, above and below the cooperative ordering of Nd ions taking place in $NdFeO_3$ at $T_{N2}=1.05$ K. Above T_{N2} (which is always the case in $NdCrO_3$), the Zeeman splitting of the ground doublet can be written as

$$\Delta_g=2(-\mu_z^{Nd}H_{Nd-Cr}+J_{Nd}\eta), \tag{6}$$

where J_{Nd} is the exchange constant of the Nd-Nd interaction, and η is a dimensionless mean-field parameter describing the magnetic-induced order of Nd in the c_z (Γ_1) mode. Neutron diffraction[32] shows that η can be neglected at T_{SRT}. Moreover, H_{Nd-Cr} can be considered temperature independent below ~ 50 K, because the Cr subsystem is fully saturated, as shown by the entropy curve S_{Cr} of Fig. 7. Thus, with the values $\mu_z^{Nd}=1.93\pm 0.3\mu_B$ and $\Delta_g/k_B=27.15$ K, an effective exchange field can be obtained: $H_{Nd-Cr}=105\pm 12$ kOe. This value is in quite good agreement with that obtained in Ref. 13. In the framework of the mean-field approximation, H_{Nd-Cr} is generated by the ordered magnetic moments of Cr,

$$H_{Nd-Cr}=n_{Nd-Cr}G_y=\frac{1}{4S}n_{Nd-Cr}\mu_{Cr}\hat{G}_y, \tag{7}$$

where $S=3/2$, $\hat{G}$ is Bertaut's combination of 3/2 spins, and $\mu_{Cr}=2.9\ \mu_B$ in $NdCrO_3$.[10] At the temperatures of interest, the Cr system is fully saturated (i.e., $\hat{G}_y=4S$), and we obtain a value for the Nd-Cr mean-field interaction parameter: $n_{Nd-Cr}=H_{Nd-Cr}/\mu_{Cr}=36\pm 4$ kOe/μ_B.

The phenomenological interaction parameter n_{R-M} can be compared from one RMO_3 system to another, as it is independent of the magnitude of the magnetic moments of the rare-earth and transition-metal ions. In particular, it is interesting to compare it with n_{Nd-Fe} in $NdFeO_3$, as it has been published that the interaction is more than one order of magnitude larger in the chromite than in the ferrite.[13,16] In Ref. 8 we obtained $H_{Nd-Fe}=66$ kOe from the fitting of specific-heat and neutron-diffraction experiments. This value takes into account Nd-Fe and Nd-Nd interactions as well as the Van Vleck susceptibility. In analogy to Eq. (7), using the value $\mu_{Fe}=4.6\mu_B$ (Ref. 37) yields $n_{Nd-Fe}=14.4$ kOe/μ_B in $NdFeO_3$. As a consequence, the interaction strength ratio between the two compounds is $n_{Nd-Cr}/n_{Nd-Fe}=2.6$. Thus, although the Nd-M interaction is actually stronger in the chromite than in the ferrite, the ratio cannot be considered anomalous within the dispersion in the RMO_3 family. The different Δ_g values of several systems along the series illustrate this point. For example, in $NdNiO_3$, the average of the two Nd sites gives $\Delta_g^{NdNi}/k_B=4.7$ K, similar to $NdFeO_3$. Recent specific-heat measurements on $NdMnO_{3+\delta}$ allowed

us to determine $\Delta_g^{NdMn}/k_B = 23 \pm 2$ K.[38] Similar differences appear in other rare earths, for example, $SmFeO_3$ has $\Delta_g^{SmFe}/k_B = 22.5$ K, $SmCrO_3$ has $\Delta_g^{SmCr}/k_B = 8$ K, $HoFeO_3$ has $\Delta_g^{HoFe}/k_B = 8$ K, $HoCrO_3$ has $\Delta_g^{HoCr}/k_B = 16$ K, etc. (see Ref. 1 for more examples).

The ratio $n_{Nd\text{-}Cr}/n_{Nd\text{-}Fe}$ was clearly overestimated in previous literature.[13,16] The problem lies in the smallness of the Zeeman splitting obtained by Hornreich and Yaeger by fitting magnetization and magnetic susceptibility data in $NdFeO_3$: $\Delta_g^{NdFe}/k_B = 1.6$ K.[39] The difference with the experimental value of $\Delta_g/k_B = 5.7$ K (Ref. 40) was ascribed to Nd-Nd interaction. This has been demonstrated to be a wrong statement, as $J_{Nd}/k_B = 0.825$ K in $NdFeO_3$,[8] and $2J_{Nd}\eta/k_B$ remains smaller than 2 K even at $T \approx 1$ K, when η reaches its value of saturation [$\eta(0) = 1.15$].

In conclusion, our work solves the riddle of the origin of the strength of Nd-Cr interaction. The Nd-Cr interaction in the chromite is stronger than the Nd-Fe one in the ferrite by (only) a factor ~ 2.6, which has to be attributed to different superexchange Nd-M paths, i.e., Nd-M distances, Nd-O-M angles, and electronic overlapping. In the experimentally measurable magnitude directly related to Nd-M interaction, Δ_g, the Nd-Cr interaction strength, greater than the Nd-Fe interaction strength, is enhanced by the fact that the Nd magnetic moment in the chromite is approximately twice that in the ferrite. The single-ion anisotropy of Nd (originating the magnitude of the Nd magnetic moment and the g tensor) arises from the particular wave functions of the Nd ground doublet, which are due to a crystal field acting on the Nd ion and are peculiar to each system.

It would appear interesting to compare quantitatively the relative strengths of the exchange integrals of the Cr-Cr, Nd-Cr, and Nd-Nd interactions, i.e., to translate $n_{Nd\text{-}Cr}$ into the $J_{Nd\text{-}Cr}$ appearing in an isotropic Heisenberg-like Hamiltonian $-2J_{Nd-Cr}\Sigma \mathbf{S}_{Nd}\mathbf{S}_{Cr}$. This is not the correct treatment for Nd-Cr interaction: the isotropic R-M exchange in orthorhombic perovskites is only due to the weak ferromagnetic components, and, in particular, it vanishes in the purely antiferromagnetic Γ_1 phase. The phenomenological $n_{Nd\text{-}Cr}$ is fully due to anisotropic and antisymmetric (non-Heisenberg) exchange.[41]

The very important role played by non-Heisenberg exchange in the magnetic properties of RMO_3 perovskites was put into evidence, by Yamaguchi,[33] among others, who, looking for a satisfactory theory of spin reorientation transitions, developed a model which takes into account isotropic, anisotropic, and antisymmetric terms of the R^{3+}-M^{3+} interactions. The model neglects the R^{3+} single-ion anisotropy, based on two facts: spin reorientations take place at relatively high temperatures in most RMO_3 systems, and they can be also observed in compounds where M is the isotropic Gd^{3+} ion. Yamaguchi's approach succeeds in describing continuous and abrupt reorientation transitions in every RMO_3 (M = Fe, Cr) system except $NdCrO_3$. In the cited work, Yamaguchi concluded that Nd^{3+} single-ion anisotropy plays a very important role in the spin reorientation transition and low-temperature magnetic properties of this compound. Our work confirms his conjecture.[42–44]

ACKNOWLEDGMENTS

This work was supported by the MAT97-0987 and MAT99-1142 CICYT and the INTAS 97-10177 projects. We thank Dr. A.M. Kadomtseva for the single crystal of $NdCrO_3$ used in the experiments.

[1] P. Pataud and J. Sirvardière, J. Phys. (France) **31**, 1017 (1970).
[2] F. Bartolomé, M. D. Kuz'min, R. I. Merino, and J. Bartolomé, IEEE Trans. Magn. **30**, 960 (1994).
[3] F. Bartolomé, M. D. Kuz'min, J. Bartolomé, J. Blasco, J. García, and F. Sapiña, Solid State Commun. **91**, 177 (1994).
[4] F. Bartolomé, Ph.D. thesis, Universidad de Zaragoza, 1995.
[5] I. Plaza, E. Palacios, J. Bartolomé, S. Rosenkranz, C. Ritter, and A. Furrer, Physica B **234**, 632 (1997).
[6] I. Plaza, E. Palacios, J. Bartolomé, S. Rosenkranz, C. Ritter, and A. Furrer, Physica B **234**, 635 (1997).
[7] E. F. Bertaut, in *Magnetism*, edited by G. T. Rado and H. Suhl (Academic Press, New York, 1963), Vol. 1.
[8] J. Bartolomé, E. Palacios, M. D. Kuz'min, F. Bartolomé, I. Sosnowska, R. Przenioslo, R. Sonntag, and M. M. Lukina, Phys. Rev. B **55**, 11 432 (1997).
[9] J. L. García Muñoz, J. Rodríguez Carvajal, and P. Lacorre, Phys. Rev. B **50**, 978 (1994).
[10] E. F. Bertaut and J. Mareschal, Solid State Commun. **5**, 93 (1967).
[11] J. B. Ayasse, A. Berton, and J. Sivardiere, C. R. Seances Acad. Sci., Ser. B **271**, 1220 (1970).
[12] E. F. Bertaut, J. Mareschal, G. de Vries, R. Aleonard, R. Pauthenet, J. P. Rebouillat, and J. Sivardiere, IEEE Trans. Magn. **2**, 453 (1966).
[13] R. M. Hornreich, Y. Komet, R. Nolan, B. M. Wanklin, and I. Yaeger, Phys. Rev. B **12**, 5094 (1975).
[14] R. M. Hornreich, Y. Komet, and B. M. Wanklin, Solid State Commun. **11**, 969 (1972).
[15] N. Shamir, M. Melamud, H. Shaked, and S. Shtrikman, Physica B **90**, 217 (1977).
[16] K. P. Belov, M. A. Belyanchikova, A. M. Kadomtseva, I. B. Krinetskii, T. M. Ledneva, T. L. Ovchinnikova, and V. A. Timofeeva, Fiz. Tverd. Tela (Leningrad) **14**, 248 (1972) [Sov. Phys. Solid State **14**, 199 (1972)].
[17] J. Bartolomé and F. Bartolomé, Phase Transit. **64**, 57 (1997).
[18] A. R. Miedema, R. F. Wielinga, and W. J. Huiskamp, Physica (Amsterdam) **31**, 1585 (1965).
[19] H. A. Algra, L. J. de Jongh, W. J. Huiskamp, and R. L. Carlin, Physica B **92**, 187 (1977).
[20] W. Marti, M. Medarde, S. Rosenkranz, P. Fisher, A. Furrer, and C. Klemenz, Phys. Rev. B **52**, 4275 (1995).
[21] F. Lindemann, Z. Phys. **11**, 609 (1910).
[22] A. Podlesnyak, S. Rosenkranz, F. Fauth, W. Marti, A. Furrer, and A. Mirmels. J. Phys.: Condens. Matter **5**, 8973 (1993).
[23] C. A. Morrison and R. P. Leavitt, in *Handbook on Physics and Chemistry of the Rare Earths*, edited by K. A. Gschneidner, Jr. and L. Eyring (North-Holland, Amsterdam, 1982), Chap. 46, and references therein.

[24] R. Kubo, Phys. Rev. **87**, 568 (1952).
[25] M. Lowenhaupt, Physica B **163**, 479 (1990).
[26] S. Rosenkranz, M. Medarde, F. Fauth, J. Mesot, M. Zolliker, A. Furrer, U. Staub, P. Lacorre, R. Osborn, R. S. Eccleston, and V. Trounov, Phys. Rev. B **60**, 14 857 (1999).
[27] J. S. Kouvel and H. Brooks (unpublished).
[28] J. van Kranendonk and J. H. van Vleck, Rev. Mod. Phys. **30**, 1 (1958).
[29] G. S. Rushbrooke and P. J. Wood, Mol. Phys. **1**, 257 (1958).
[30] J. P. van der Ziel and L. G. van Uitert, J. Appl. Phys. **40**, 977 (1969).
[31] Y. Endoh, K. Kakurai, A. K. Katori, M. S. Seehra, G. Srinivasan, and H. P. J. Wijn, *Perovskites II: Oxides with Corundum, Ilmenite, and Amorphous Structures*, Landolt-Börnstein, New Series, Group 3, Vol. 27, Pt. f3 (Springer-Verlag, Berlin, 1994)
[32] N. Shamir, H. Shaked, and S. Shtrikman, Phys. Rev. B **24**, 6642 (1981).
[33] T. Yamaguchi, J. Phys. Chem. Solids **35**, 479 (1974).
[34] The energy values when perfoming this calculation have to be shifted by $\Delta_g/2$, as the energy origin is the center of gravity of the former ground doublet.
[35] F. Bartolomé, J. Bartolomé, and JR. S. Eccleston, J. Appl. Phys. **87** (2000).
[36] M. Eibschtz, L. Holmes, J. P. Maita, and L.G.v. Uitert, Solid State Commun. **8**, 1815 (1970).
[37] W. C. Koehler, E. O. Wollan, and M. K. Wilkinson, Phys. Rev. **118**, 58 (1960).
[38] F. Bartolomé, J. Bartolomé, and J. Blasco (unpublished).
[39] R. M. Hornreich and I. Yaeger, Int. J. Magn. **4**, 71 (1973).
[40] M. Loewenhaupt, I. Sosnowska, and B. Frick, J. Phys. (Paris), Colloq. **12**, 49-C8 (1988).
[41] K. P. Belov, A. K. Zvezdin, and A. M. Kadomtseva, Sov. Sci. Rev., Sect. A **9**, 117 (1987).
[42] C. Kapusta and P. C. Riedi, in *NMR Studies of Intermetallics and Interstitial Solutions Containing H, C, and N*, Vol. 281 of *NATO Advanced Studies Institute Series E: Interstitial Intermetallic Alloys*, edited by F. Grandjean, G. J. Long, and K. H. J. Buschow (Kluwer, Dordrecht, 1995), Chap. 20.
[43] Y. Berthier, M. Boge, G. Czjzek, D. Givord, C. Jeandey, H. S. Li, and J. L. Oddou, J. Magn. Magn. Mater. **54-57**, 589 (1986).
[44] S. Kobayashi, N. Sano, and J. Ito, J. Phys. Soc. Jpn. **21**, 1456 (1995).